

Enhanced magnetization of nanoscale colloidal cobalt particles

J. P. Chen, C. M. Sorensen, and K. J. Klabunde

Department of Physics, Kansas State University, Manhattan, Kansas 66506

G. C. Hadjipanayis

Department of Physics & Astronomy, University of Delaware, Newark, Delaware 19716

(Received 10 November 1994)

We have used a microemulsion technique to synthesize metallic cobalt particles in the size range 18 to 44 Å diameter. The particles are spherical, not aggregated due to their surfactant coating, and free of oxide. Magnetic properties such as total moment per particle, blocking temperature, and hysteresis all show reasonable size dependencies. The effects of small size are seen in: (1) the anisotropy constant increased markedly as particle size decreased, and (2) the total magnetic moment per atom in the Co particles was enhanced with decreasing particle size by as much as 30% over the bulk value. Magnetization versus applied field curves indicate the particles are heterogeneous with two magnetic phases, possibly a core-shell structure. The core phase has a large total moment and the shell phase is superparamagnetic with an effective moment of $7.5 \pm 1\mu_B$ for all sizes. We propose that the shell phase is responsible for the enhanced anisotropy and magnetization.

I. INTRODUCTION

The magnetic properties of bulk ferromagnetic materials have been widely studied and relatively well understood. For particles the extrinsic magnetic properties, such as hysteresis behavior, superparamagnetism, and domain structure, have also been well studied and understood. Still lacking, however, are sufficient investigations of intrinsic magnetic properties, such as magnetization, anisotropy, and Curie temperature of fine particles, to develop a clear understanding of the bulk to atomic transition. A major problem in this effort has been to develop synthetic techniques capable of producing large quantities of very small and chemically homogeneous particles.

The earliest reported studies on the size dependence of the saturation magnetization of nanoscale particles involved ensembles of particles. Luborsky and Lawrence¹ claimed that the saturation magnetization of ultrafine Fe particles as small as 15 Å in diameter dispersed in mercury and frozen in liquid nitrogen was almost the same as that of bulk iron. On the other hand, Tamura² found the hyperfine field coming from the interfacial Fe atoms in oxidized Fe particles to be 8% larger than that of bulk Fe, indicating a larger moment for Fe surface atoms. Furubayashi³ found that 20 Å average diameter Fe particles, free from oxidation, had a 3% increase in saturation magnetization. The average hyperfine field of the Fe particles was also 3% larger than that of bulk, which corroborated the magnetic measurement. Any study of nanosized particles must insure against surface oxidation, which is particularly a problem for iron, which can cause the total magnetization to be smaller.⁴

Recently there has been a considerable amount of work involving the properties of single, gas-phase atomic clusters of the transition metals whose magnetic moments were measured with a Stern-Gerlach apparatus.⁵⁻⁹ Iron, cobalt, and nickel all show ~30% enhancements in the

magnetic moments per atom as the number of atoms per cluster falls from several hundred to a few tens of atoms. Rhodium, paramagnetic in the bulk, becomes ferromagnetic for clusters of 31 atoms or less.⁸ These particles should be free of interfacial interactions, thus one can conclude that size can strongly affect the magnetization. This enhancement has been ascribed to the surface atoms which become the dominant phase as size declines and for which the electronic structure has been altered because of the different symmetry compared to the bulk.¹⁰⁻¹³

In this paper we describe an inversed micelle synthesis of ultrafine cobalt particles in the size range 18 to 44 Å in diameter. Hysteresis measurements show that their surface is not oxidized and electron microscopy shows that they are not aggregated. We find the anisotropy constant of these particles increases dramatically from the bulk value as size decreases. We also find as much as a 30% enhancement of the saturation magnetization for our smallest particles. Magnetization versus field graphs indicate two different magnetic phases for each particle. One phase has a fairly large moment and behaves ferromagnetically below a blocking temperature. The other phase is roughly superparamagnetic for $T > 2$ K with an effective moment of $7.5 \pm 1\mu_B$. We argue that this two-phase behavior is due to a core-shell structure of the particles.

II. EXPERIMENTAL METHOD

The inversed micelle technique is an established chemical method for synthesizing metallic particles.^{14,15} In this work, Co particles were synthesized in the binary system of DDAB/toluene,¹⁶ where DDAB(didodecyldimethylammonium bromide) is a cationic surfactant. Sodium borohydride, NaBH_4 , was used to reduce CoCl_2 to obtain Co particles. First $\text{CoCl}_2 \cdot 6\text{H}_2\text{O}$ was dissolved in an 11

wt. % DDAB solution in toluene at concentrations of 0.005 to 0.02 M. The reagent was trapped in the empty micelles and formed a blue transparent solution. Then a 10 M NaBH_4 aqueous solution was added with the condition of $[\text{BH}_4^-]:[\text{Co}^{2+}] = 3:1$ and stirred vigorously. In approximately 2 min the mixture turned from blue to black and formed a stable colloid. To study the magnetic properties, the toluene was evaporated completely with Co particles and DDAB left behind, which formed a powder sample. Before the reaction, both solvents, water, and toluene, were deoxygenated by bubbling with Ar gas. The whole process was carried out in a glove bag filled with Ar gas to prevent oxidation of the Co particles.

The magnetic properties were measured with a Quantum Design superconducting quantum interference device (SQUID) magnetometer. Roughly 100 mg samples were contained in a gelatin capsule and then placed in the SQUID. The He gas boil off kept the samples protected from oxygen.

When we studied the temperature dependence of the spontaneous magnetization σ at low field for zero-field-cooled samples, we found that the particles were not pure metallic cobalt when the mole ratio of water to DDAB was much larger than one. Figure 1 shows the data for two samples with the same preparation except the water content. In sample *A* 60 μl of 5 M NaBH_4 , whereas in sample *B* 30 μl of 10 M NaBH_4 , was added to 10 ml of 0.01 M CoCl_2 solution in DDAB/toluene. Sample *A* shows two peaks in the σ vs T plot in Fig. 1, while its magnetization was just 50% of that of sample *B*, which had only one peak in that plot. The two peaks imply two magnetic phases in sample *A*. In nonmicroemulsion systems we have shown^{17,18} how water causes the borohydride reduction to create Co_2B whereas Co is created in the absence of water. Thus we interpret the results for

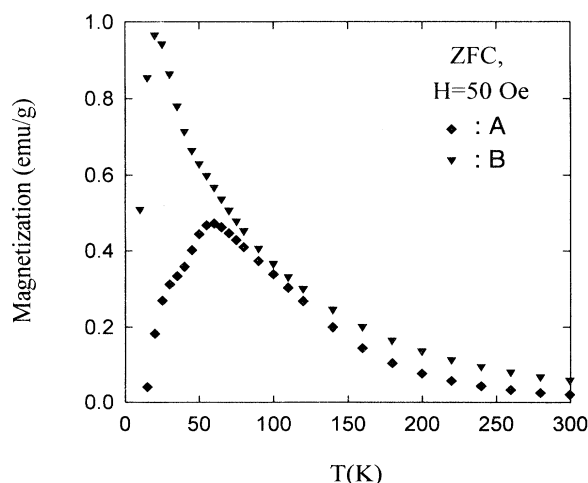


FIG. 1. Temperature dependence of the spontaneous magnetization at $H = 50$ Oe for zero-field-cooled samples *A* and *B*. In sample *A* 60 μl of 5 M NaBH_4 , whereas in sample *B* 30 μl of 10 M NaBH_4 was added to a 0.01 M $\text{CoCl}_2 \cdot 6\text{H}_2\text{O}$ solution in DDAB/toluene. The peak at 20 K in both *A* and *B* is due to Co, the peak at 60 K in *A* is due to Co_2B .

sample *A* to imply that both Co and Co_2B particles were produced. On the other hand, in sample *B* only Co is produced. There was, of course, water present in sample *B*, but at low concentration (one H_2O molecule per DDAB molecule in sample *B*). The water must be fixed by the hydrophilic part of the DDAB and unable to participate in the Co reduction. We remark that Pileni *et al.*¹⁹ found the oxidation states of metallic copper particles changed with the change of water content in the micelles.

With the above results in mind, we controlled the ratio of $[\text{H}_2\text{O}]:[\text{DDAB}]$ below 1.5 to make pure metallic cobalt. The particle size was varied by changing the CoCl_2 concentration in the DDAB/toluene system from 0.005 to 0.02 M. We have also tried to increase the particle size by increasing of reaction temperature to 50°C, but no obvious change was observed.

III. RESULTS

Figure 2 is a transmission electron microscopy (TEM) picture of the particles and shows that the cobalt particles are uniformly distributed in the DDAB matrix. This uniformity and the fact that their average spacing (120 Å) is roughly twice the length of the surfactant molecules implies that the individual particles are coated with a monolayer of the surfactant molecules. No aggregation is observed. The particles are spherical and have a narrow size distribution. The average particle diameter could be varied from 18 to 44 Å by varying the CoCl_2 concentration from 0.005 to 0.02 M.

The x-ray diffractogram of a powder sample showed only the (111) peak of fcc cobalt. Since the concentration of cobalt in the sample is about 0.6 wt. %, the other weaker peaks were in the noise. Previous work^{20,21} showed that fcc, instead of hcp as in the bulk, was the stable structure of Co particles.

It is well known that Co particles coated with CoO will exhibit exchange anisotropy due to interfacial interaction between ferromagnetic Co metal and antiferromagnetic CoO.^{4,22} In these systems the hysteresis loops will be dis-

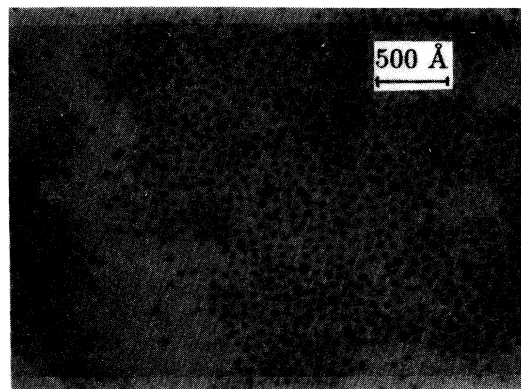


FIG. 2. TEM photograph of the cobalt particles with an average particle diameter of 33 Å.

placed along the field axis if they are cooled in a magnetic field. Figure 3 shows the hysteresis loop of a Co sample measured at 10 K after the sample was cooled in a field of 10^4 Oe. The loop is symmetric about zero field. The center of the loop is just 15 Oe from zero point, compared to a coercivity of 1084 Oe and within the experimental error limit of zero. The symmetry implies that no CoO was formed on the particle surfaces. The Co particles were free from oxidation.

Low-field ($H = 50$ Oe) susceptibility χ measurements are shown in Fig. 4. The diamagnetic susceptibility of the DDAB was measured and subtracted to obtain these results. Above the blocking temperature, the inverse susceptibility is roughly linear with temperature in accord with the Curie law. At high temperatures, where the susceptibility is small this linearity breaks down. We believe this is due to a strongly temperature-dependent saturation magnetization which decreases the particle's superparamagnetic moment, hence increases the slope of χ^{-1} vs T , at large temperature. Overall Fig. 4 suggests the particles are superparamagnetic above the blocking temperature and their effective moment per particle increases with increasing size.

The Co samples showed a consistent set of magnetic properties measured by the SQUID magnetometer. Shown in Fig. 5 are the size dependences of the magnetic moment per Co particle, magnetic size, blocking temperature, and coercivity. The magnetic moment per particle was calculated from the susceptibility χ in Fig. 4 above the blocking temperature at low field according to Eq. (1)

$$\chi = \frac{\sigma_s \mu}{3k_B T}, \quad (1)$$

where μ is the magnetic moment per particle, σ_s is the saturation magnetization, and k_B is Boltzmann's constant. Using the total saturation magnetization at high field (see below) and μ , we derived the magnetic particle sizes from the magnetic data, which are shown in Fig. 5(b). The magnetic size is consistent with the TEM size

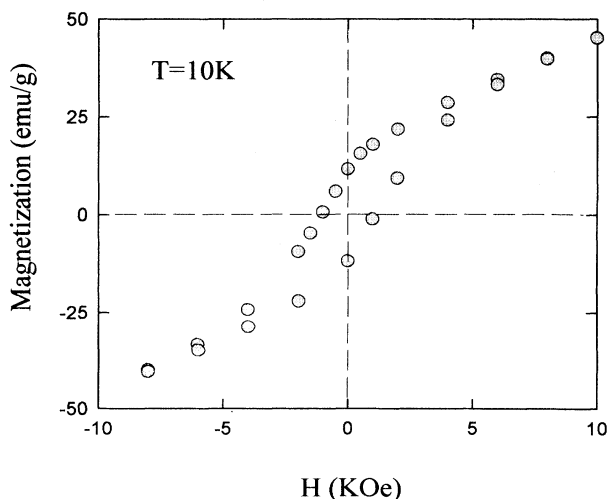


FIG. 3. Hysteresis loop at 10 K of a Co sample with an average diameter of 33 Å.

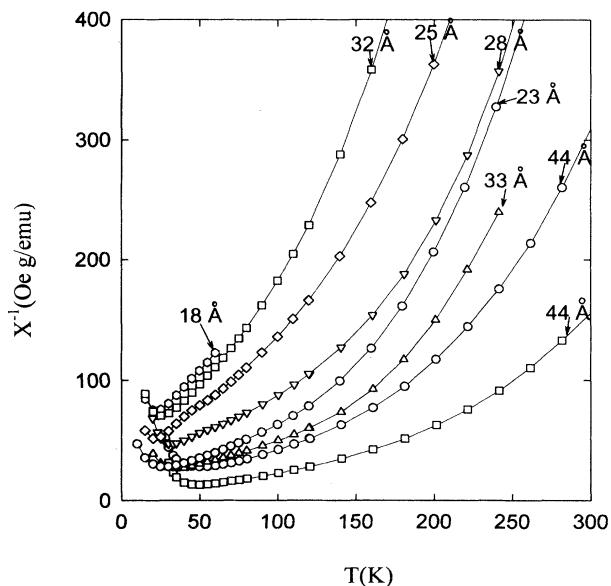


FIG. 4. Inverse susceptibility versus temperature for various sized Co particles.

but systematically larger for as yet unexplained reasons. The blocking temperature was measured when warming the zero-field-cooled sample in a field of 50 Oe, an example of which is given in Fig. 1. It increased as particle size increased as expected. As the particle size increased, their coercivity also increased as expected for particles with size smaller than the single-domain size. All the properties are consistent with the typical behavior of fine particles, which implies a series of good samples.

The Co particles showed an enhanced anisotropy constant as they become smaller as shown in Fig. 6. The anisotropy constant K was determined from the blocking temperature and particle volume as²²

$$K = 30k_B T/V. \quad (2)$$

The volume V was calculated from the TEM size. All the values of K were above that of bulk fcc Co (2.7×10^6 erg/cm³).^{23,24} As the particle size decreased, the anisotropy constant increased. There are several possible reasons for the enhancement. One is that CoO exists on the surface, but as we showed above, there was no oxidation layer. Another possible source of increased anisotropy is shape anisotropy. But the TEM shows our particles to be fairly spherical. Therefore the most reasonable explanation is surface anisotropy. As we know, there is a large fraction of Co atoms on the surface for nanometer-sized particles. These atoms can have a large anisotropy,²⁵ which in turn causes the total anisotropy energy to be enhanced. Finally, stress anisotropy may have some contribution to the total value, but we have no means to estimate its effect.

Magnetization σ versus applied field H is shown in Fig. 7 and versus H/T in Fig. 8 for $d = 33$ Å particles. These curves are typical for all sizes. We interpret these curves to be the result of two different magnetic phases. Phase 1 saturates by $H \approx 10$ kOe to the value of ~ 30 emu/total

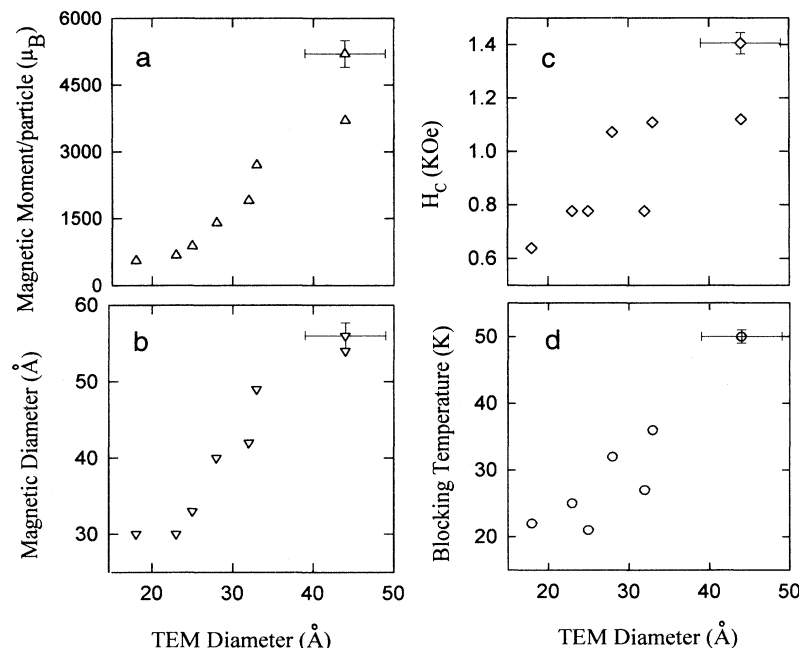


FIG. 5. Magnetic behavior of the Co particles. (a) Magnetic moment per particle determined from the susceptibility using Eq. (1). (b) Particle diameter determined from σ_s and magnetic moment. (c) Size dependence of the coercivity at 10 K. (d) The blocking temperature as a function of particle size.

gram of Co. It is ferromagnetic below the blocking temperatures of Fig. 5(d) and has a large effective moment as indicated in Fig. 5(a). Phase 2 is roughly paramagnetic as indicated by Fig. 8 and its magnetization adds to phase 1 to yield the curves in Fig. 7.

An important issue is where these two phases are physically located. Phase 1 is associated with the large magnetic moments and the blocking temperatures and hence is part of the particles. Comparison of the relative magnetizations at high field and low temperature indicates that phase 2 is the majority phase. X-ray fluorescence measurements indicate that there is no Co in the matrix between the particles, thus phase 2 must be associated

with the particles as well. We conclude that each particle is heterogeneous with both phases present. How are these phases configured? Both the high-temperature behavior, where the magnetization due to phase 2 is small, and extrapolation of σ at large H down to $H=0$ indicate saturation magnetization values for phase 1 of 12 to 30 emu/total gram of cobalt, and these values increase roughly with particle size as shown in Fig. 9. This behavior is consistent with a core-shell model in which the core is phase 1 and the shell is phase 2 with a constant thickness. If phase 1 has $\sigma_s = 166$ emu/g, the bulk value, then the shell would have a thickness of ~ 7 Å for all particles sizes.

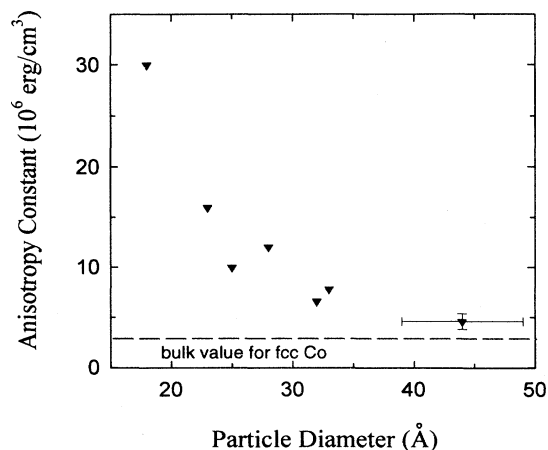


FIG. 6. Anisotropy constant of Co particles as a function of particle size.

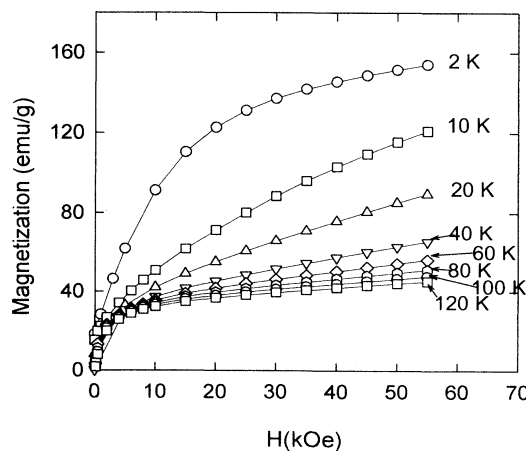


FIG. 7. Magnetization as a function of applied field at different temperatures for Co particles with an average diameter of 33 Å.

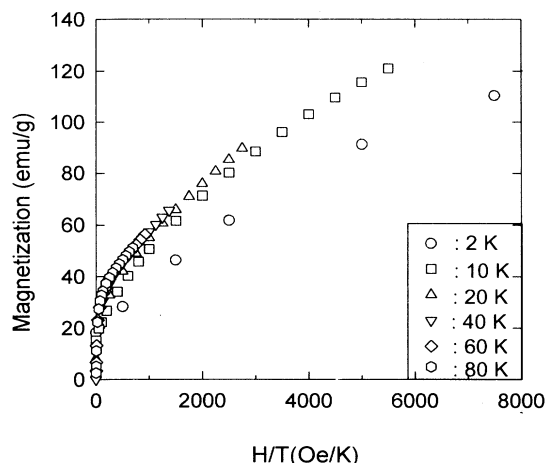


FIG. 8. Magnetization as a function of applied field divided by temperature for Co particles with an average diameter of 33 Å.

The implication that chemically homogeneous metallic particles are magnetically heterogeneous with a core-shell structure is similar to the recent conclusions of others. Billas, Châtelain, and de Heer⁹ interpreted their magnetic data for gas-phase clusters for Fe, Co, and Ni to imply that the inner atoms had bulk magnetic moments, but atoms near the surface did not. Mulder *et al.*²⁶ claimed for Pt clusters that the inner core displayed “metallic” character like that of the bulk whereas the surface did not. A generalization of core-shell structure for metallic particles is not unreasonable given the breaking of symmetry at the surface.

Phase 2 shows universal behavior of σ vs H/T for $T > 10$ K to imply paramagnetism. For $T \leq 10$ K the curves do not overlap well but are much closer than when plotted versus H . The moment implied by this Curie law behavior is $7.5 \pm 1 \mu_B$. This value is either too big or too small depending on one’s point of view. It is too big to be

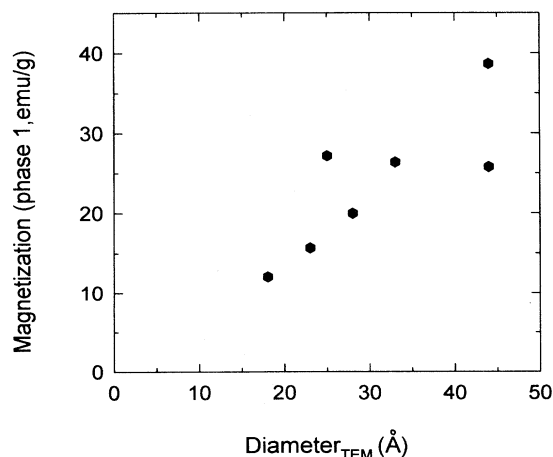


FIG. 9. Saturation magnetization of phase 1 as a function of particle diameter.

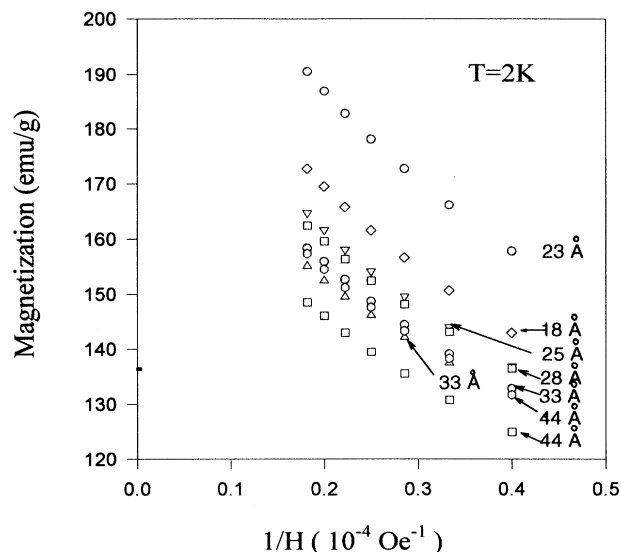


FIG. 10. Magnetization at 2 K as a function of $1/H$ for eight different samples.

single cobalt atoms ($1.7 \mu_B$ when ferromagnetic, $3.13 \mu_B$ for $T > T_c$) or ions ($3 \mu_B$ for Co^{+2}). It is too small when one considers that phase 2 is a larger fraction of the cobalt than phase 1 and the effective superparamagnetic moment of phase 1 is on the order of 10^3 [Fig. 5(a)]. If the atomic moments in phase 2 acted coherently as a superparamagnetic, then the moment of phase 2 should be greater than the moment of phase 1, which it is not. Thus at this time we were unable to explain the moment of $7.5 \mu_B$.

The high-field behavior of the Co particles is also seen in Fig. 7. The particles are not saturated at 2 K and 5.5 T. Shown in Fig. 10 are the magnetic data for eight Co samples at 2 K with $1/H$ as the abscissa axis. The satura-

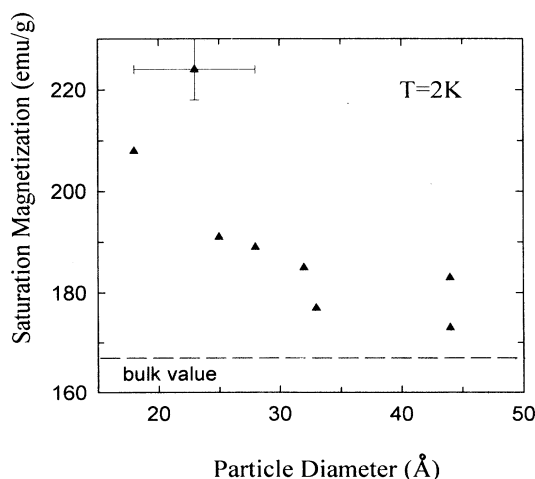


FIG. 11. Saturation magnetization of Co particles at $T = 2$ K (bulk $\sigma_s = 166$ emu/g).

tion magnetizations obtained from the extrapolation of Fig. 10 as $1/H \rightarrow 0$ are shown in Fig. 11. As the particle size decreases, the saturation magnetization increases. All the saturation values are above the value of the bulk fcc Co material [166 emu/g (Ref. 27) or 175 emu/g (Ref. 28)].

The enhanced saturation magnetization implies an enhanced magnetic moment per atom qualitatively consistent with results obtained for free Co clusters and Fe and Ni clusters in general.⁵⁻⁹ Our particles range in average diameter from 18 to 44 Å. Assuming the same density of cobalt atoms as in the bulk, these sizes correspond to $N=280$ to 4000 atoms per particle. The latest gas-phase cluster results for Co indicate an enhancement does not begin until $N \leq 400$.⁹ For $N=280$ the enhancement is $\sim 10\%$. Thus the enhancements are qualitatively similar but do not match quantitatively. Our particles are coated with surfactant which must interact with them in some manner since the TEM, Fig. 2, shows them still coated with the surfactant. The gas-phase clusters have a free surface. This difference may be the cause of the magnetic difference. At this time we cannot determine what effect this surfactant layer might have on the magnetic

properties. Further experiments are needed to clarify this possible effect.

IV. CONCLUSIONS

Microemulsion synthesis of nanoscale Co particles has been shown to yield reasonably monodisperse, spherical, unaggregated and unoxidized particles. The magnetic anisotropy and saturation magnetization are size dependent and both increase above bulk values as the particle size decreases. Magnetization versus applied field curves indicate two magnetic phases associated with each particle possibly in a core-shell morphology. The nature of the core is probably similar to the bulk. The shell phase, has an effective moment which is too large to be associated with single atoms but much too small to represent the whole phase. It is reasonable to propose that the enhanced anisotropy and magnetization are due to this shell phase whose fraction increases with size decrease.

ACKNOWLEDGMENT

This work was supported by NSF Grant No. 9013930.

- ¹F. E. Luborsky and P. E. Lawrence, J. Appl. Phys. **32**, 2315 (1961).
- ²I. Tamura and M. Hayashi, Surf. Sci. **146**, 501 (1984).
- ³T. Furubayashi, I. Nakatani, and N. Saegusa, J. Phys. Soc. Jpn. **56**, 1855 (1987).
- ⁴G. C. Hadjipanayis, S. Gangopadhyay, C. M. Sorensen, and K. J. Klabunde, IEEE Trans. Magn. **29**, 2602 (1993).
- ⁵W. de Heer, P. Milani, and A. Châletain, Phys. Rev. Lett. **65**, 488 (1990).
- ⁶J. P. Bucher, D. C. Douglass, and L. A. Bloomfield, Phys. Rev. Lett. **66**, 3052 (1991).
- ⁷D. C. Douglass, A. J. Cox, J. P. Buckner, and L. A. Bloomfield, Phys. Rev. B **47**, 12 874 (1993).
- ⁸A. J. Cox, J. G. Louderback, and L. A. Bloomfield, Phys. Rev. Lett. **71**, 923 (1993).
- ⁹I. M. L. Billas, A. Châletain, and W. A. de Herr, Science **265**, 1682 (1994).
- ¹⁰J. Merikoski, J. Timonen, M. Manninen, and P. Jena, Phys. Rev. Lett. **66**, 938 (1991).
- ¹¹S. N. Khanna and S. Linderorth, Phys. Rev. Lett. **67**, 742 (1991).
- ¹²S. Linderorth and S. N. Khanna, J. Magn. Magn. Mater. **104-107**, 1574 (1992).
- ¹³R. V. Reddy, S. N. Khanna, and B. I. Dunlap, Phys. Rev. Lett. **70**, 3323 (1993).
- ¹⁴M. Boutonnet, J. Kizling, P. Stenius, and G. Maire, Colloid. Surf. **5**, 209 (1982).
- ¹⁵J. P. Wilcoxon, United States Patent, No. 5147841, 1992.
- ¹⁶J. P. Chen, C. M. Sorensen, K. J. Klabunde, and G. C. Hadjipanayis, J. Appl. Phys. **75**, 5876 (1994).
- ¹⁷G. N. Glavee, K. J. Klabunde, C. M. Sorensen, and G. C. Hadjipanayis, Langmuir **8**, 771 (1992).
- ¹⁸G. N. Glavee, K. J. Klabunde, C. M. Sorensen, and G. C. Hadjipanayis, Inorg. Chem. **32**, 474 (1993).
- ¹⁹M. P. Pileni, J. Phys. Chem. **97**, 6961 (1993).
- ²⁰M. E. Mohenry, S. A. Majetich, J. O. Artman, M. DeGraef, and S. W. Staley, Phys. Rev. B **49**, 11 358 (1994).
- ²¹W. Gong, H. Li, Z. Zhao, and J. Chen, J. Appl. Phys. **69**, 5119 (1991).
- ²²B. D. Cullity, *Introduction to Magnetic Materials* (Addison-Wesley, New York, 1972).
- ²³W. D. Doyle and P. J. Flanders, *International Conference on Magnetism, Nottingham, 1964* (The Institute of Physics and the Physical Society, Bristol, 1965), p. 751.
- ²⁴W. A. Sucksmith and J. E. Thompson, Proc. R. Soc. London **225**, 362 (1954).
- ²⁵F. Bodker, S. Morup, and S. Linderorth, Phys. Rev. Lett. **72**, 282 (1994).
- ²⁶F. M. Mulder, T. A. Stegink, R. C. Thiel, L. J. de Jongh, and G. Schmid, Nature (London) **367**, 716 (1994).
- ²⁷M. Nishikawa, E. Kita, T. Erata, and A. Tasaki, J. Magn. Magn. Mater. **126**, 303 (1993).
- ²⁸J. R. Childress and C. L. Chien, Phys. Rev. B **43**, 8089 (1991).

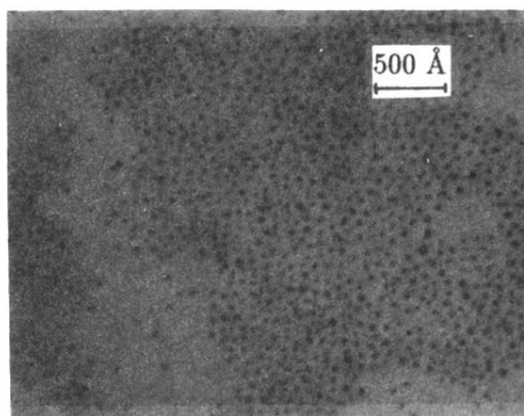


FIG. 2. TEM photograph of the cobalt particles with an average particle diameter of 33 Å.